Sensors and Actuators A 152 (2009) 219–233

Contents lists available at ScienceDirect

Sensors and Actuators A: Physical

journal homepage: www.elsevier.com/locate/sna

Review

Piezoelectric ultrasonic micro/milli-scale actuators

B. Watson, J. Friend*, L. Yeo

Monash University, Department of Mechanical and Aerospace Engineering, Micro/Nanophysics Laboratory, Clayton, VIC 3800, Australia

ARTICLE INFO

Article history:
Received 7 October 2008
Received in revised form 13 March 2009
Accepted 2 April 2009
Available online 10 April 2009

PACS:
07.10.Cm
85.50. −n
43.35.+d
89.75.Da

Keywords:
Piezoelectric
Micro-actuator
Micro-motor
Ultrasonic
Review

ABSTRACT

A growing demand for actuators with a volume of less than 1 mm^3 has driven researchers to produce a varied range of micro/milli-scale designs. By examining the underlying physics of the actuator operation we are able to demonstrate why piezoelectric ultrasonic actuators have the greatest potential to meet this need. Moreover, it allows us to create a new classification system for piezoelectric ultrasonic actuators, affording us a better understanding of the core characteristics of each class of actuator, which class is most suited to various applications, and highlights potential areas of future research.

Contents

1. Introduction

There is growing demand for actuators with a volume of less than 1 mm^3. This need has been reported across the micro-robotics industry [1] and the medical profession [2,3]. Despite such varied fields of use, the core characteristics required of actuators at millimetre and sub-millimetre scales are the same. Actuators at these scales require high output forces, accuracy, low response times, a simple design and simple operation. An understanding of how well myriad actuator classes may meet these requirements can be determined by examining the underlying physics of the actuator operation. The key focus of such an investigation is the force that is

* Corresponding author.
E-mail address: James.Friend@eng.monash.edu.au (J. Friend).

0924-4247/$ – see front matter © 2009 Elsevier B.V. All rights reserved.
doi:10.1016/j.sna.2009.04.001

Table 1
Comparative scaling of motor driving forces (F is output force, L is characteristic length).

Motor class	Driving force	Scaling
Electromagnetic	Electromagnetic	$F \propto L^4$
Electrostatic	Electrostatic	$F \propto \frac{1}{L^2}$
Thermal	Mechanical strain	$F \propto L$
Osmotic	Osmotic effect	Dependent on many variables
ECF	ECF	$F \propto \frac{1}{L}$ minimum
Piezoelectric ultrasonic	Converse piezoelectric effect	$F \propto L$

used as the basis of design. This is the force that is produced by the stator and induces motion in the rotor/slider; hereafter referred to as the driving force.

Electromagnetic actuators are the most widely used of any design at the macro-scale, with small-scale versions also having been developed [4,5]. The driving force for an electromagnetic actuator relies on the interaction of the permanent magnets of the rotor, and the magnetic field induced by the current in the coil of the stator. The use of this non-destructive, non-contact force gives the electromagnetic actuator a high energy density, which compares favorably with most other actuator designs and has led to its wide spread use. However, as detailed in Table 1, the electromagnetic force poorly scales down [6] and the relative performance of an electromagnetic actuator becomes progressively worse as the length scale reduces to the order of millimetres. Moreover, due to the reduction in scale the electromagnetic driving force promotes an undesirable high speed, low force behaviour in the actuator. We concluded from this that the driving force that makes an electromagnetic actuator superior to most actuators in large-scale applications likewise makes it unsuitable as the actuator volume is reduced to the desired 1 mm^3.

The simple design of the electrostatic actuator has enabled researchers to produce actuators with diameters as small as 100 μm [7] and beyond [8], making them among the smallest practical actuators produced. This small size has led to some success in the field of micro-electro-mechanical systems (MEMS) [9], where size is of critical importance. As with electromagnetic actuators, electrostatic actuators use a non-contact force to create mechanical work. The force arises from the interaction between charged materials, and decreases with the square of the distance between the two charged bodies. The excellent scalability of the electrostatic force (the force increases with a reduction in size, see Table 1), is a major design advantage, and has allowed the development of the very small-scale actuators previously noted. However, the electrostatic driving force also leads to the disadvantages associated with these designs. Most importantly, the electrostatic driving force is weak when compared with many other forces used for actuation and in spite of excellent scaling characteristics, limits the output of electrostatic actuators. At the scales noted previously, the output torque is currently limited to approximately 10 pNm [7]. The electrostatic driving force also results in a nonlinear output for the actuator. This is particularly problematic at the end of the output range, where actuators can undergo 'snap-down'. Moreover, the electrostatic driving force is very sensitive to the operating environment and actuator design. The maximum electrostatic field strength is strongly dependent on humidity and ambient gas content and the force performs best with actuator designs with low aspect ratios (large electrode surface compared to distance to travel). These deficiencies are less important for many MEMS applications, but limit the actuator's use in most other areas.

Thermal actuators are another actuator design that have been employed in MEMS applications [10,11]. This type of design can be produced at scales comparable to electrostatic actuators, but have output forces in the order of micro-Newtons. In contrast to electromagnetic and electrostatic actuators, thermal actuators use a mechanical strain, rather than a non-contact force, as a driving force. Mechanical strain rates greatly vary depending on the type of material used, with smart memory alloys (SMAs) having significantly higher strain rates than regular metallic alloys. Regardless of the material used, the output can be magnified through clever geometric design with the actuator performance scaling linearly due to the inherent thermal characteristics. Although the thermally induced mechanical strain of these designs produces a high output force and scales well, actuators that use this driving force have two significant disadvantages. The first is that the driving force used results in a response time that is very slow when compared to alternatives, also affecting the actuator velocities obtained from the designs. The second is that the lifespan of the actuator may be limited due to the plastic strain arising from repeated cycling. With such characteristics, thermal actuators are most suited to applications that require large forces infrequently, such as micro-grippers.

Osmotic actuator designs utilise a different approach to creating motion [12] than those actuator classes already covered. The removal of the need for an electrical input is advantageous for some operating conditions and the design has obvious benefits for use with microfluidics. The driving force of an osmotic actuator is the increase in pressure within a vessel, leading to an expansion of an actuation diaphragm. The increased pressure is caused by one-directional flow of liquid across a semi-permeable diaphragm, driven by the osmotic effect. How well an osmotic actuator can be scaled is dependent on many factors, including the diaphragm material used and the concentration of the osmotic agent. Osmotic actuators have numerous disadvantages when applied to a broad spectrum of applications including:

- Slow response times, leading to low actuator velocities.
- Complex designs required obtain large, linear or rotational outputs.
- Problems with solute deposition, fouling and control.

Such drawbacks demonstrate that osmotic actuators are unsuitable for many applications. It is worthy to note however, that like thermal actuators, osmotic actuators have shown potential for use as micro-grippers.

A further somewhat unusual design is the design developed by Yokota et al. [13,14]. The driving force of these motors is the jetting phenomenon induced in an electro-conjugate fluid (ECF) when in the presence of an electric current. The motors use a rotor with vanes to harness the ECF jetting, producing the output rotation. Although the ECF jetting phenomenon is not yet fully elucidated, it has been demonstrated that motors designed using this driving force improve in performance as the scale is reduced [13]. Motors of these designs have good outputs, and excellent scalabilty, however, there may be difficulties in further reducing the scale of these motors below 1 mm^3 [15].

The first piezoelectric ultrasonic micro/milli-scale actuators evolved from earlier larger scale piezoelectric actuators successfully used in cameras [16]. Since then, numerous small-scale actuators have been produced, including designs with dimensions of only a few millimetres [17] and nanometre positioning accuracy [18]. The driving force of a piezoelectric actuator arises from the converse piezoelectric effect, which converts a harmonic electrical input to a cyclic strain in the piezoelectric element. This driving force scales linearly with the characteristic length scale, potentially allowing useful amounts of work to be produced from small-scale actuators. This is especially true when the actuators are designed to operate near the mechanical resonance of the stator. In addition to good scalability, piezoelectric actuators have numerous other benefits for use as milli/micro-actuators. They include:

- Large output torques
- Direct drive
- No gearbox or brake mechanism required
- Bearingless
- Quick response
- No backlash
- Negligible effects from external magnetic fields
- Simple design
- Low voltages

The drawback of current piezoelectric ultrasonic resonant actuators include a significant performance loss if a deposited piezoelectric material is used for very small scales (see actuators produced by Morita et al. as an example [20,21]) and the potential complexity of the control system due to multiple input signals required by most designs.

The underlying physics of the actuator operation demonstrates that piezoelectric ultrasonic actuators have the greatest potential to meet the core requirements of an actuator design as devices are reduced in scale below 1 mm^3 in volume.

This paper reviews piezoelectric ultrasonic actuators that have made significant steps towards reaching the goal of a true micromotor. In addition, we introduce a classification system that forms the structure of our review. By using the underlying physics of the actuator design as the basis for the classification, we are able to encompass previously proposed classification systems [22,23], whilst promoting a better understanding of the core characteristics of the proposed design. Moreover, the use of such a classification system aids in determining which piezoelectric ultrasonic actuator class is best suited to various applications and highlights potential areas of future research.

2. Commonalities of piezoelectric ultrasonic micro/milli-scale actuators

The focus of this paper is to review piezoelectric ultrasonic micro/milli-scale actuators by examining the differences in their underlying physics of operation. To enable this to be completed successfully, it is prudent to first cover the commonalities shared by all piezoelectric ultrasonic actuators.

The first and most important of these is that piezoelectric materials are the basis for all piezoelectric ultrasonic resonant actuators. The piezoelectric element in actuators may be used in bulk form as the stator [24], as a method to induce vibration in the stator [18], or in a deposited form [21].

Piezoelectricity, from the Greek *piezein*, means squeeze or pressure electricity. The general definition of piezoelectric materials is that they develop an electric charge differential along an axis of piezoelectric polarisation if placed under appropriate mechanical strain (direct piezoelectric effect) and deform if an electric field is applied along the same axis of polarisation (converse piezoelectric effect). Piezoelectric materials may be used to provide static and dynamic deformations, at frequencies up to several gigahertz, depending on the motion to be induced, the scale of the device, and the material used.

As previously noted, actuators make use of the converse piezoelectric effect as a driving force. The converse piezoelectric effect arises when, upon the application of an electric field to a piezoelectric material, a dipole moment is created by the relative motion of the material's atoms. This motion may contract or expand the unit cell, leading to a maximum strain in the piezoelectric element of approximately 1%.

Upon the application of an electric field, for the atom motion to occur the piezoelectric material must be non-centrosymmetric in crystal structure, and be polarised. Non-centrosymmetric refers to the lack of a centre of symmetry in the crystal structure. Materials which are centrosymmetric, when placed under stress, exhibit a symmetrical movement, inhibiting the formation of a mechanical strain. As an example, Fig. 1 shows the centrosymmetric (non-piezoelectric) and non-centrosymmetric (piezoelectric) crystal structure of barium titanate. Most piezoelectric materials are generally not naturally polarised, nor polarised by the fabrication process. To polarise the material, an applied electric field or mechanical strain is used. For an in-depth examination of these materials for use in piezoelectric actuators, see the work by Kenji Uchino [25].

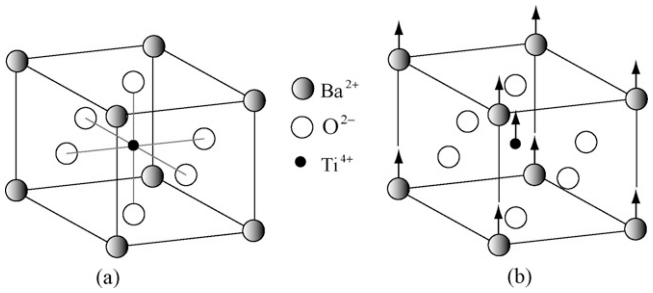

Fig. 1. The (a) centrosymmetric (non-piezoelectric) and (b) non-centrosymmetric (piezoelectric) crystal structure of barium titanate. Note the offset barium and titanium atoms.

We can also note the generalised operation of a piezoelectric ultrasonic resonant micro/milli-scale actuator is to convert the cyclic motion of the piezoelectric element to a net work at the rotor or slider. This is achieved through a friction coupling between the stator and rotor or slider.

The stator design and the physics harnessed by it during operation are the key things we are to examine in Sections 3 through 6. Here we note that the goal of all stator designs is to produce an elliptical motion at the stator tip (the point of contact between the stator and rotor/slider). As demonstrated by Fig. 2, an elliptical stator tip motion is desirable as it results in the stator imparting both a contact (normal) and driving (tangential) force on the rotor or slider, resulting in the desired stator/rotor output.

In reality, it is very difficult to obtain the idealised motion as illustrated in Fig. 2. It is far more common to keep the stator or rotor in constant contact with the stator. This ensures that the output obtained is repeatable for each stator cycle. The method by which this achieved is known as the friction coupling and is the other key commonality among piezoelectric ultrasonic actuators. The principle of the friction coupling is to ensure that a larger contact force is exerted between the rotor/slider and the stator for one half of the operating cycle than the other half. Using a coulombic friction model, we can see that the cyclic contact force leads to a cyclic frictional force which, when time averaged across one stator cycle, results in a net work at the rotor/slider in a given direction. This leads to a net motion of the rotor or slider. We can see this illustrated in Fig. 3.

To ensure this constant contact force, a preload is used. This is a normal force on the rotor or slider in the opposite direction to that imposed by the stator and is usually a magnetic, weight or spring force.

Although the friction coupling ensures a repeatable output, it is also the area of greatest inefficiency in a piezoelectric ultrasonic actuator. Only a small part of the energy within the stator is converted to a useful net tangential displacement of the rotor. The remaining energy is wasted through the unused motion of the rotor and in heat, caused by friction.

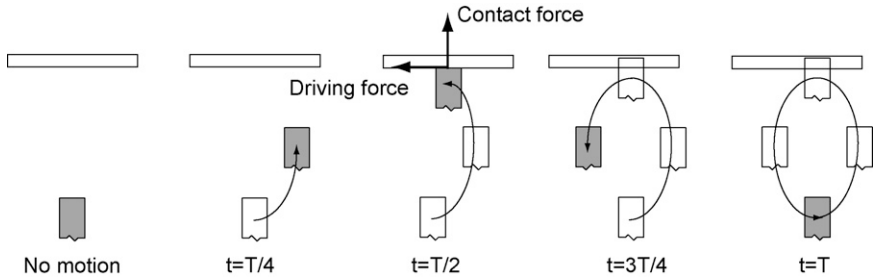

Fig. 2. The idealised stator tip motion for one cycle for a piezoelectric ultrasonic actuator. The elliptical stator tip motion enables the stator to impart both a contact (normal) and driving (tangential) force on the rotor or slider, resulting in the rotor/slider being driven through friction. Note: *T* is period and *t* is cycle time.

3. Piezoelectric ultrasonic actuator classification

As noted in Section 2 the key differentiation in the design of piezoelectric ultrasonic actuators is the method by which the stator converts the motion of the piezoelectric elements to the elliptical stator tip motion. By analysing these methods, we can develop a classification system which affords us a clearer understanding of the advantages and disadvantages associated with a specific design, allows a selection of a particular actuator class best suited to an application, and enables better comparison of actuator performances. It may also highlight potential areas of future research needed to meet a specific need. Piezoelectric ultrasonic actuators can be classified according to:

- the type of wave used to promote motion,
- the type of motion being produced by the actuator,
- the vibration mode, if any, being induced in the stator, and
- how vibration modes of the stator are being combined.

Fig. 4 shows a delineation of the different actuators into these classes.

For the remainder of this paper we use this classification system to review existing piezoelectric ultrasonic micro/milli-scale actuators. We describe the different operational principles used within the design of each class, how these relate to the characteristics and performance of the actuator, and highlight examples of each class.

4. Standing wave piezoelectric ultrasonic micro/milli-scale actuators

Standing wave actuators make use of resonant vibration modes to elicit the elliptical motion from the stator. This motion may be one [24], or several stator tips [26]. The elliptical motion may be created by coupling different resonant modes (i.e., coupled orthogonal bending, coupled axial and bending, or coupled axial and torsional) through the use of multiple piezoelectric elements or through a combination of resonant mode and geometrical design.

The use of resonant vibration modes as the basis of design for this class of actuator governs the common performance characteristics. Specifically, the comparatively large outputs achieved by this class of actuators are a result of the amplification of the piezoelectric strain achieved under resonant conditions. The magnitude of this effect varies with the vibration mode used, as we will explore later, and scales linearly with the characteristic length of the piezoelectric element. This accounts for the excellent scalability of these designs. The resonant conditions of the stator also determine the speed of operation. Counter-productively, operating at resonance can reduce the service life of the actuator, requiring additional consideration during design.

4.1. Rotational actuators

4.1.1. Flexural mode actuators

Flexural mode actuators are designed to use a flexural resonant mode of a thin, flat (membrane-like) stator. The stator, in general, is fabricated from or coated with a piezoelectric material, with the resonant mode excited by the direct application of an alternating electric field.

The flexural resonant mode-shape of the membrane-like stator results in a linear stator displacement. To obtain the required elliptical motion from the stator, a geometric addition must be made to the "membrane". This geometric addition will modify the linear motion of the stator surface to create a elliptical path for the stator tip. An example is the actuator produced by Dubois and Muralt [29], as shown in Fig. 5, which uses 'elastic fins' attached at regular positions under the rotor. During the upward phase of the flexural mode in the membrane-like piezoelectric stator, the fins do not slide when pushed by the stator, owing to friction, but bend elastically. Due to the 'tilt angle' at which the fins are fixed, this action results in a horizontal movement of the rotor. During the downward phase of the stator, when the friction force is small, the fins relax and follow the rotor.

Although actuators in this class are operated at a resonant mode, the magnitude of displacement in the stator caused by a flexural wave is small. This limits the output that can be produced by such designs. As an example, the design produced by Dubois and Muralt achieved a maximum torque of 0.94 μNm, from an actuator with a diameter of 5.2 mm. The excitation frequency of this mode is also relatively low, leading to comparatively slower rotational speeds.

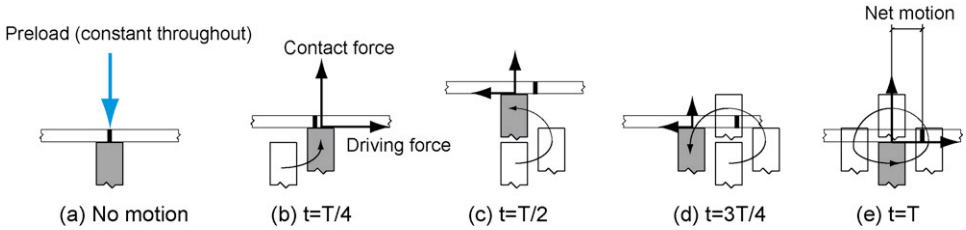

Fig. 3. By applying a "preload" to the slider/rotor, it remains in contact during the stator for the complete cycle, ensuring a repeatable output. The elliptical motion now ensures a greater contact (and hence driving force) is applied during part of the cycle (b) and (e), than the other (c) and (d), resulting in a net motion.

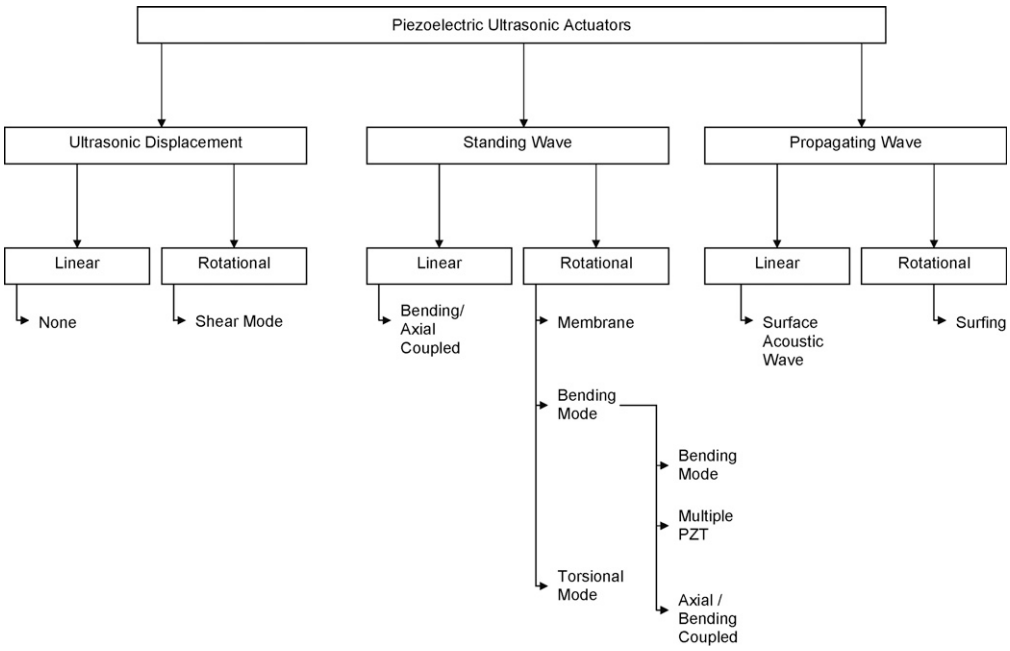

Fig. 4. Classes of piezoelectric ultrasonic milli/micro-actuators as determined by the examination of the underlying physics of actuator operation.

Dubois and Muralt reached a peak rotational velocity of 1020 rpm at an input of 70.6 kHz.

These operational characteristics, derived from the driving force, mean that flexural mode standing wave actuators are well suited to low speed, low output applications where packaging is of primary concern. An example of such an application is in watches, where the flat geometry and reliable motion is more important than the actuator performance.

4.1.2. Bending mode actuators

By far the largest group of piezoelectric ultrasonic micro/millis-cale actuator designs are those that use resonant bending modes. Designs in this class excite a first-order bending mode in combination with another vibration mode to achieve the desired elliptical stator output. This combination may be two orthogonal first-order bending modes, or a first-order bending mode and an unrelated mode (i.e., an axial vibration mode).

First-order bending modes produce the largest stator tip displacement of any mode-shape. This has a direct and beneficial effect on the performance of the actuator, promoting a high torque output for a given size. The use of first-order bending modes also has an effect on the output speed of the design. In general, first-order bending modes are excited at lower frequencies than other modes (i.e., axial or torsional). As such, the operating frequency will be lower, resulting in a lower output rotational velocity than alternative designs.

The most widely researched bending mode designs are those that use orthogonal bending modes to create an elliptical stator tip motion. Known as "wobble motors", the name is derived from the appearance of the stator during operation. In these designs, the actuator may be driven using one [17] or multiple piezoelectric elements [30].

To demonstrate the wobble motion, we consider a simple beam fabricated from a piezoelectric material, as shown in Fig. 6. The first-order orthogonal bending modes, bending modes *1* and *2*, of the beam in Fig. 6 can be isolated by driving the piezoelectric element at the correct frequencies. We assume a harmonic electrical input to the piezoelectric element and no proportion of any other mode effecting the beam motion. If the beam is driven at the natural frequency that excites bending mode *1*, the displacement of point *A* on the stator tip in the *x*-direction is given by

$$u_x(t) = u_0 \sin(\omega t + \alpha), \tag{1}$$

where u_0 is the magnitude of vibration, ω is the frequency of vibration, t is the time and α is the phase constant. There is no motion in the *y*-direction for bending mode *1*. Similarly, if we drive the beam at the natural frequency of bending mode *2*, the displacement of point *A* on the stator tip in the *y*-direction is given by

$$u_y(t) = u_1 \sin(\omega t + \beta), \tag{2}$$

where u_1 is the magnitude of vibration, ω is the frequency of vibration, t is the time and β is the phase constant. There is no motion in the *x*-direction for bending mode *2*. If we now consider these two

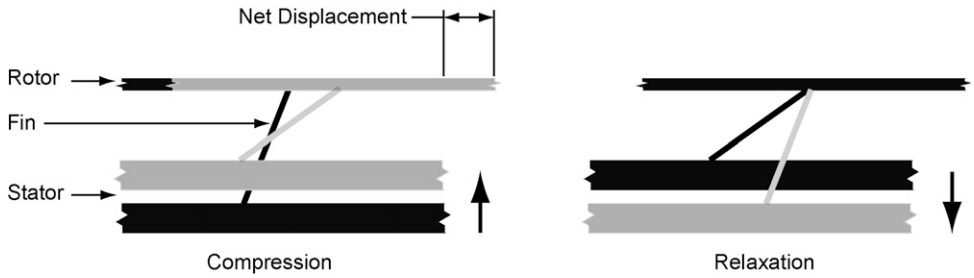

Fig. 5. The membrane actuator by Dubois and Muralt [29] uses 'elastic fins' to convert the linear motion of the piezoelectric "membrane" to the desired elliptical motion.

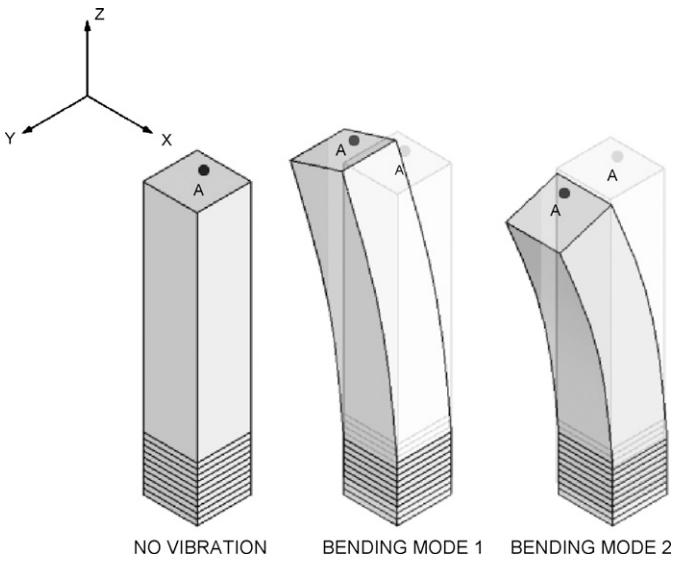

Fig. 6. The first-order stator orthogonal bending modes excited during the operation of a bending mode actuator.

bending modes to be excited simultaneously, the motion of point A can be considered to be the combination of Eqs. (1) and (2). Together these equations describe an elliptical path in the x–y plane.

If we also include the change in position in the z-direction due to the effects of bending during this excitation, the displacement at point A can further be described by

$$u_z(t) = u_2 \sin(\omega t + \gamma), \tag{3}$$

where u_2 is the magnitude of vibration, ω is the frequency of vibration, t is the time and γ is the phase constant. The path trace of point A can then be sketched as shown in Fig. 7.

The simplest of these designs uses a single piezoelectric stator with multiple electrodes. These multiple electrodes allow two driving signals to be used simultaneously, creating orthogonal bending modes. The actuator is designed to run at the fundamental bending mode of the stator. It is excited by four electrical sources, with $\pm 90^\circ$ phase shifts. By reversing the phase shifts, the rotation direction can also be reversed.

The first use of this design at the milli-scale was reported by Morita et al. [19]. The design uses a thin-film PZT (9 μm) deposited by a hydrothermal method on to the surface of a titanium tube, 2.4 mm in diameter and 10 mm in length. Electrodes were then formed

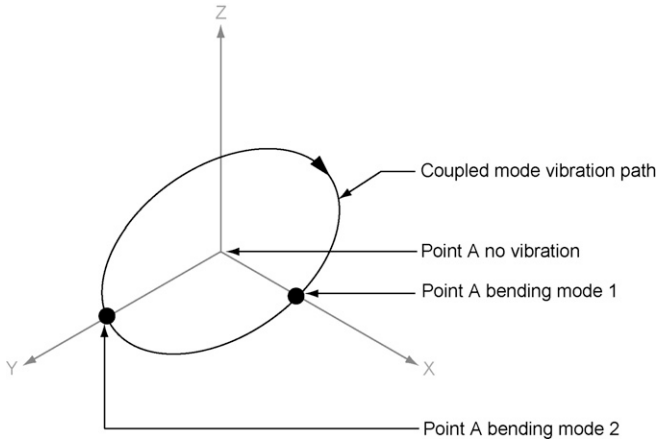

Fig. 7. The theoretical trace of the stator tip of a bending mode actuator for one period. The elliptical motion is achieved by coupling orthogonal first-order bending modes.

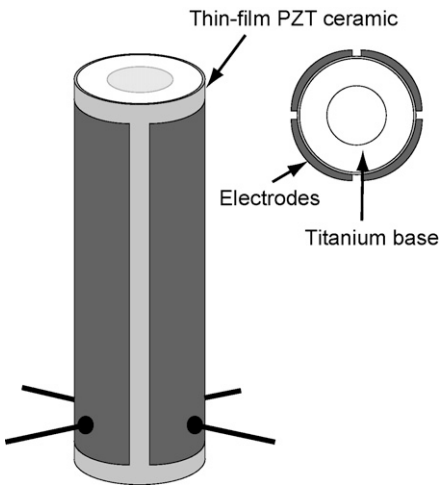

Fig. 8. The early bending mode actuator by Morita et al. [19] uses multiple electrical inputs to a cylindrical stator with a thin-film piezoelectric coating, to simultaneously excite orthogonal bending modes. Note the four external electrodes.

in four places on the PZT layer. This is detailed in Fig. 8. The motor achieved bi-directional operation and a peak rotation of 295 rpm with a driving voltage of 20–33 V_{p-p}.

This design was subsequently advanced by Morita et al. in 2000 [21]. The thin-film PZT was increased to 12 μm in thickness, deposited using the hydrothermal method on a titanium base as before. The stator dimensions were reduced to 1.4 mm in diameter and 5 mm in length. The actuator was driven at the first bending mode resonant frequency of the stator of 227 kHz. The maximum rotational velocity was 680 rpm with a maximum torque of 0.67 μNm.

Morita et al. also modified this design, to produce one of the first micro/milli-scale actuator designs to use a bulk piezoelectric element as the stator. The actuator has a cylindrical stator, 2.4 mm in diameter and 10 mm in length. The stator consists of a bulk cylindrical PZT element, a single cylindrical inner electrode and four outer electrodes, as shown in Fig. 9. The PZT is poled through the thickness from the outside to the inside. The actuator housing holds the stator through rubber O-rings at two nodal positions and the rotor is preloaded by a spring.

The driving frequency for the actuator is 85 kHz, which produced a maximum rotational velocity of 650 rpm. The input voltage was 100 V_{p-p} and the actuator produced a maximum torque of 220 μNm. The maximum efficiency was 25%, which is excellent for an actuator of this scale. As an example of future applications, the

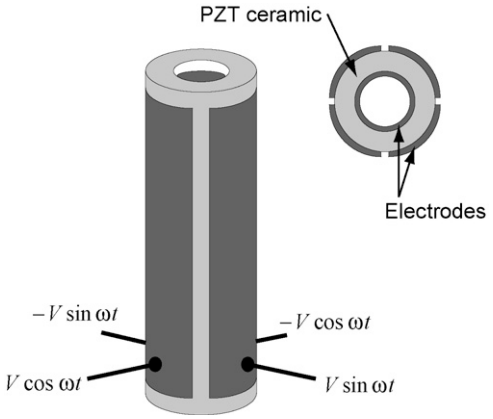

Fig. 9. Morita et al. [20] also applied the design from Fig. 8 to a bulk PZT stator. Here the earth electrode is internal.

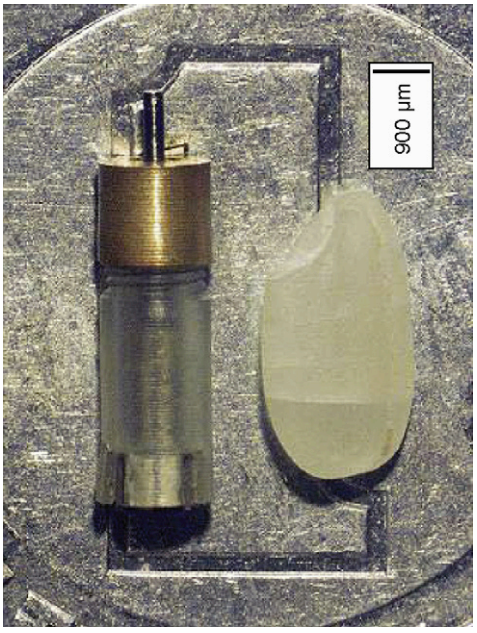

Fig. 10. An image of a "wobble motor" by Kanda et al. [17]; note the small size of the motor when compared to the grain of rice on the right. (Figure © [2004] IEEE).

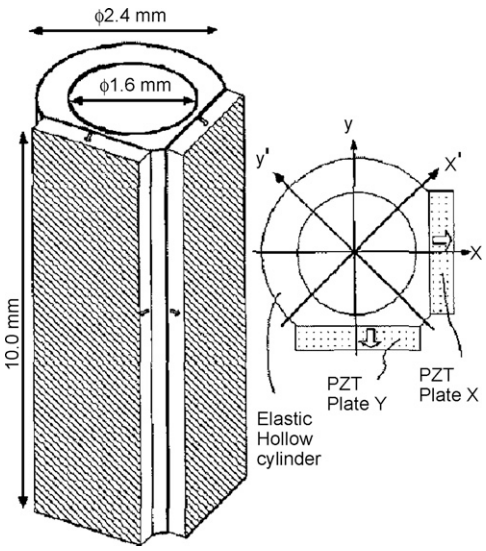

Fig. 11. When excited by one of the piezoelectric elements, the degenerate bending modes of the bending mode actuator by Koc et al. [30] couple to create an elliptical motion at the stator tip. Excitation by the second piezoelectric element reverses the rotation direction. (Figure © [2002] IEEE).

actuator was used in a 'robotic hand' and was able to drive a 10 g load [20].

The wobble motor has been scaled even further downwards. The design by Kanda et al. [17] also uses a cylindrical PZT stator and was also operated using the fundamental bending mode. The stator for this actuator is 0.8 mm in diameter and 2.2 mm in height. The total dimensions of the actuator were 2 mm in diameter and 5.9 mm in height, approximately the same dimensions as the stator design produced by Morita et al. [21]. An image of the completed actuator is shown in Fig. 10.

At 40 V_{p-p} and an operating frequency of 69 kHz the maximum rotational velocity was 3850 rpm. With a 5 mN preload, from a spring element, the maximum torque was 0.025 μNm.

A recent design in the same class was produced by Zhang et al. [24]. The dimensions of the actuator are 1 mm in diameter and 8 mm in length, including a spring element used for the preload. At a resonance frequency of 58 kHz and an input voltage of 100 V_{p-p}, the actuator produced a starting torque of 7.8 μ Nm and rotational velocities in excess of 3000 rpm.

Wobble motors produce good outputs at small scales. However, the design has limitations. The use of a bulk PZT stator, although potentially beneficial to performance, introduces possible problems in terms of reliability and robustness, due to the fragile nature of the ceramic. Moreover, the potential uses of the actuator may be limited due to the complex nature of the electrical input required for the piezoelectric element.

An alternative bending mode actuator design using two piezoelectric elements was developed by Koc et al. [30]. This actuator uses a cylinder of diameter 2.4 mm and length 10 mm, with two flattened sides which creates a mounting point for the two piezoelectric elements, as shown in Fig. 11. The piezoelectric elements were bulk PZT, poled through their thickness, with the stator itself made from brass. The actuator uses a spring element for the required preload.

The two degenerate orthogonal bending modes for such a design have a frequency that is very close, due to the symmetric structure of the stator. By exciting one piezoelectric element at a frequency between the two resonant frequencies, both modes could be excited. This resulted in the desired elliptical motion at the stator tip. By exciting the other PZT element, the rotational direction could be reversed. The actuator was operated at 69.5 kHz. At 120 V, the start-up torque was 1800 μNm. The maximum rotational velocity was 573 rpm, with a maximum power of 60 mW and a running torque of 1000 μNm. The benefit of exciting coupled resonant frequencies using one driving signal can be seen in the large output of this design. The performance of this actuator is approximately nine times better than the motor by Morita et al. [20], which is of a similar scale.

An alternative to the orthogonal bending modes used in the wobble motor, the superposition of axial and bending motions has been explored as a method for obtaining an elliptical stator motion. By exciting a bending mode in a part of the stator, whilst simultaneously vibrating the whole stator axially, an elliptical motion in the axial plane may be obtained.

As with wobble motors, the operational frequency required to excite a bending mode keeps the rotational velocity of these motors relatively low. In contrast, the vertical nature of the elliptical stator motion means that the contact point between the stator and rotor can be offset from the rotation axis of the rotor. Such a design improves the torque characteristics of this class of motor due to the increase in the moment arm associated with the stator. This is further improved by the option of having more than one contact point between the rotor and stator. However, to ensure a suitable motor scale, the size of the bending element must be reduced when compared to a wobble motor of the same scale. This reduction reduced other performance benefits, though the service life of such motors should be better than a wobble motor as the piezoelectric element does not have to be run at resonance.

A good example of such a design is the one proposed by Yao et al. [26]. This design was also one of the first piezoelectric ultrasonic resonant micro/milli-scale actuators to use a multi-layer piezoelectric linear actuator (MPLA) [31]. The MLPA is made up of hard PZT layers of a thickness of 250 μm stacked alternately with copper electrodes of 25 μm thickness and laminated with epoxy. The PZT MLPA is the largest external dimension of the actuator, with a diameter of 3 mm. This design uses two bending elements in the stator, as can be seen in Fig. 12. The actuator showed a maximum starting torque of 127.5 μNm, with a maximum rotational velocity of 1070 rpm at an input of 80 V_{p-p}.

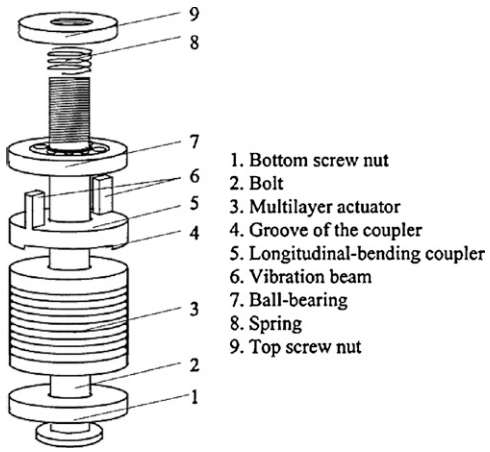

Fig. 12. The bending mode actuator by Yao et al. [26] couples the axial motion of the multi-layer piezoelectric actuator (MLPA) with the excited bending mode of the vibration beams, resulting in an elliptical stator tip motion in the vertical plane. (Figure © [2001] IEEE).

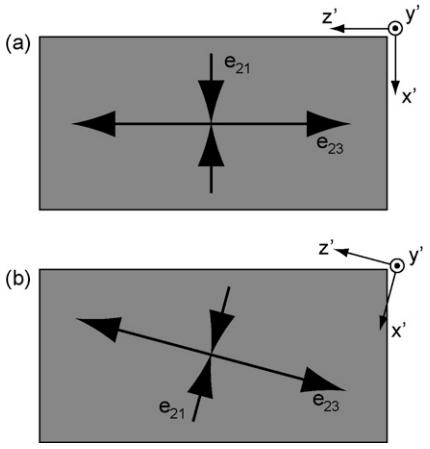

Fig. 14. An additional rotation about the y'-axis of the X-rotated, Y-plate $LiNiO_3$ allows the axial and bending resonance modes to be coupled in the actuator design by Tamura et al. [28].

A different use of bending and axial vibration modes was proposed by Suzuki et al. [32] who developed a micro-actuator 2 mm in diameter and 0.3 mm in height. The piezoelectric ceramics are shaped rectangular parallelpipeds polarised in the direction of their thickness. As the piezoelectric elements vibrate, the elastic cantilever oscillator that the piezoelectric elements are attached to generate vibration and flexion, creating elliptical movements at the free end of the cantilever oscillator. This motion is transferred to the rotor by friction with the flat spring providing a preload. The stator is constructed from PZT elements glued to a stainless steel base. The rotor is made from nickel by electroforming and gilding. The flat spring is also constructed from stainless steel, and is formed through an etching process. The actuator had an operating speed of approximately 1500 rpm with a maximum torque of 3.2 μ Nm at a driven voltage of 18 V_{p-p}.

In the design by Aoyagi et al. [27], the fundamental axial and second order bending modes of the stator are used to achieve the elliptical stator tip motion. The stator consists of two PZT elements sandwiching a stainless steel vibrator. The bending and axial modes are excited in the vibrator by the PZT elements, delivering elliptical motion at the contact point with the shaft. This is illustrated in Fig. 13. The total size of the actuator is centimetre-scale, but due to the thin shaft, and low height (approximately 50 μm) it has been included in this review. With and input of 30 V_{p-p}, this rotational actuator achieved a torque of 60 μ Nm and 8000 rpm.

Tamura et al. also produced an actuator in this class [28]. The unusual design couples the axial and bending modes in the stator by using the crystal anisotropy of Lithium Niobate ($LiNbO_3$) from which it is fabricated. Fig. 14(a) illustrates how in an X-axis rotated, Y-axis cut plate the elastic coefficients s^E_{i5} ($i = 1, 2, 3$) and the piezoelectric constant e_{25} associated with the in-plane shear are zero. This results in the fundamental axial and second bending modes being independent. However, by applying an additional rotation about the y'-axis for the standard plate (Fig. 14(b)), the elastic and piezoelectric characteristics are changed; the elastic coefficients s^E_{15} and s^E_{35} become non-zero. The longitudinal components of stress and strain in the length and width directions are combined with the in-plane shear components, coupling the fundamental axial and second bending modes. This unusual design resulted in an actuator with dimensions of 10 mm × 2.55 mm × 0.5 mm for the stator, giving a performance of 1000 rpm and 25 μ Nm in the counter-clockwise direction and 5000 rpm and 12 μ Nm in the clockwise direction.

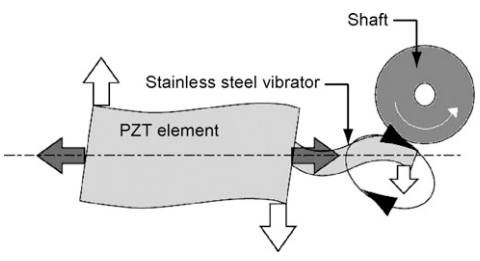

Fig. 13. The actuator by Aoyagi et al. couples the fundamental axial and second bending resonant modes within a stainless steel vibrator to impart a torque on the shaft [27].

4.1.3. Torsional mode actuators

Torsional mode actuators were one of the earliest types of piezoelectric ultrasonic actuators researched. The initial focus was on "hybrid" designs, utilising two piezoelectric elements, one poled axially and other poled radially. Using two driving signals, the output of the piezoelectric elements could be combined to create a one-directional driving force [33]. These motors, though efficient, are complex and expensive, making them unsuitable for use as a micro/milli-scale actuator.

More recent research in micro/milli-scale actuators has focussed on the coupling of torsional and axial resonant modes within the

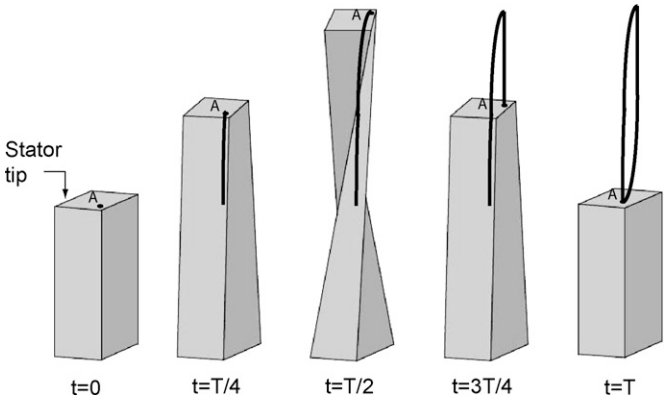

Fig. 15. An illustration of the stator motion for an axial/torsional coupled actuator, where T is the period of one cycle and t is the time. The coupling of the axial and torsional modes produces the desired elliptical stator tip motion.

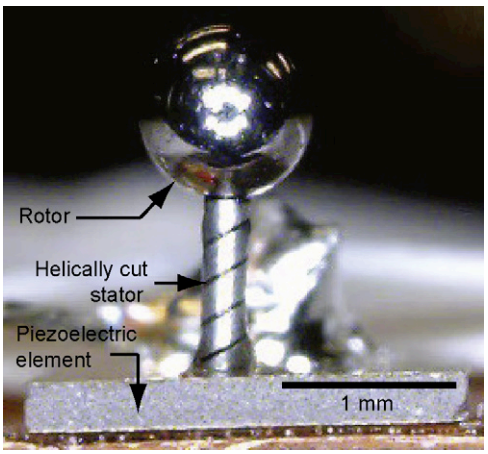

Fig. 16. Photo of the torsional mode actuator produced by Watson et al. [34]. The helical cuts in the stator couple the axial and torsional resonant modes.

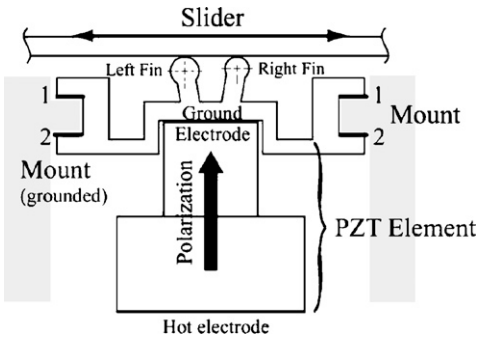

Fig. 17. Linear actuator design by Friend et al. [18]. The design uses asymmetrical fins to produce the driving force for the slider. (Figure © [2006] IEEE).

stator to achieve the same result. The axial vibration mode is used to increase or decrease the contact force between the stator and rotor, and the torsional mode is used to impart the tangential driving force. An example of a stator motion for an axial/torsional coupled mode actuator is shown in Fig. 15. The key to the design of such actuators is the geometry chosen for the stator, which enables the axial and torsional resonant modes to be matched.

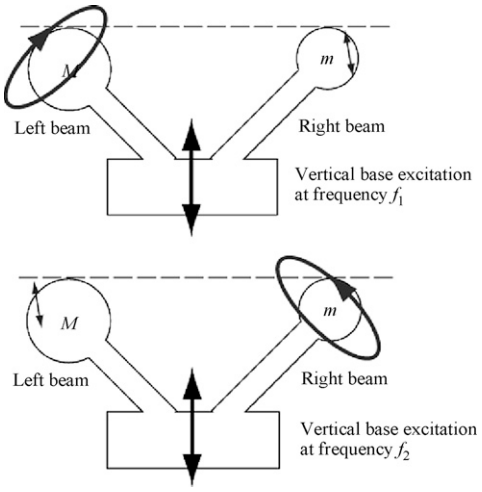

Fig. 18. The distinct resonant frequencies of the asymmetrical fins of the linear bending mode actuator by Friend et al. [18] enables bi-directional operation. (Figure © [2006] IEEE).

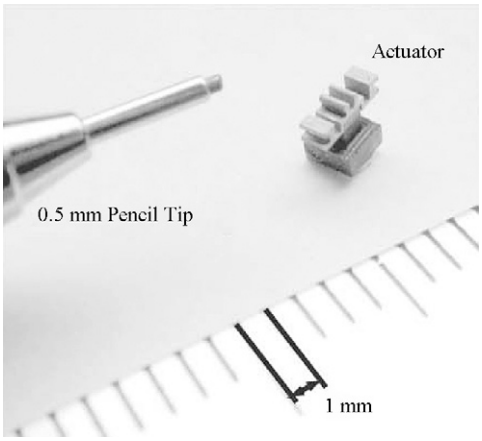

Fig. 19. A photo showing the small-scale of the "Baltan" actuator by Friend et al. [18]. (Figure © [2006] IEEE).

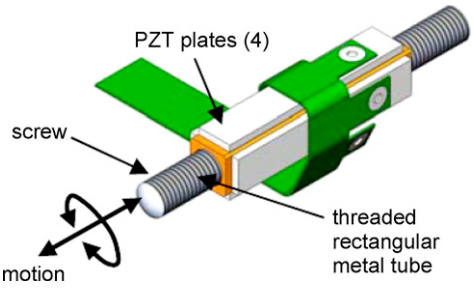

Fig. 20. The SQUIGGLE® motor by New Scale Technologies uses a small diameter threaded screw to convert the coupled orthogonal bending modes wobbling motion to a linear output [37]. (Figure © [2009] Newscale Technologies).

Both axial and torsional resonant modes produce stator tip displacements smaller than those associated with bending class actuators. However, the use of the torsional mode ensures that a large proportion of the potential tangential motion is imparted to the rotor, benefitting the actuator output. The coupled axial/torsional mode also produce higher rotational speeds than bending mode designs. The designs in general must have a long thin geometry as the stator length governs the frequency of operation. Using a short stator produces a high operating frequency, promoting undesirable operating characteristics.

The design by Watson et al. [34] is a recent example of this class of actuators and is shown in Fig. 16. Two diametrically opposed helical cuts in the stator are used to couple the axial and torsional motion of the stator tip. The stator is 250 μm in diameter and 1 mm in length, making it the smallest stator of any piezoelectric ultrasonic actuator produced. The stator is driven by a single PZT element at 677 kHz. At 28.1 V_{p-p}, the actuator produced a maximum torque of 0.013 μN-m and a maximum rotational velocity of 1300 rpm.

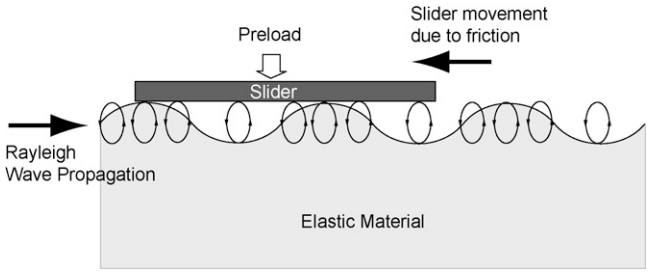

Fig. 21. Propagating wave actuators are different from standing wave actuators in that every point on the stator contact face undergoes an elliptical motion. Like standing wave actuators, friction is used to drive the slider.

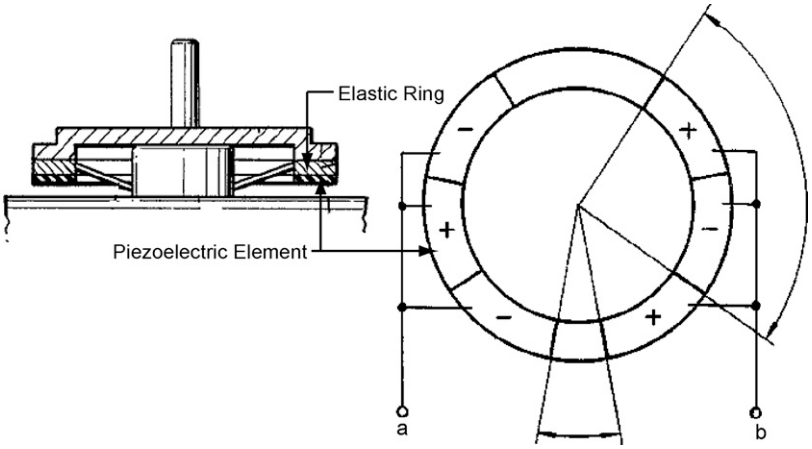

Fig. 22. A propagating wave "surfing" motor developed by Sashida [39]. The design uses multiple vibration sources (a and b) to create multiple standing waves in the piezoelectric element, that through superposition create a propagating wave around the elastic ring.

4.2. Linear actuators

Research into standing wave linear micro-actuators has been limited to designs using resonant bending modes. Linear bending mode actuators differ little in operation from rotational actuators. As with rotational actuators, a resonant bending mode of the stator is combined with another vibration mode to elicit an elliptical motion from the stator. However, due to the requirement of a linear output, it is beneficial for the stator motion to be planar, as opposed to the favoured wobble motion of rotational actuators. As such, the coupled orthogonal bending mode actuators have no particular benefits over other actuators, such as ones that employ coupled axial and bending modes.

The requirement of a two-dimensional stator motion has an effect on the characteristics of these types of actuators. As with rotational actuators, the use of a bending mode magnifies the overall displacement of the stator, benefiting the actuator output. However, as the output is linear, the disadvantage in output velocity is reduced.

One of the few linear piezoelectric ultrasonic actuators developed at millimetre scales was developed by Friend et al. in 2006 [18]. The 'Baltan' micro-actuator is a linear bi-directional micro-actuator capable of nanometre scale positioning accuracy. The stator of the actuator uses a set of asymmetrical fins to provide the driving force to the slider, as shown in Fig. 17. By changing the length, attached mass, and mounting angle of the two beams, two distinct fundamental flexural resonance frequencies can be obtained. Each beam tip, at the appropriate resonance frequency, would roughly trace out an arc centred about the beam's base due to the flexural vibration in the beam in combination with the axial motion of the base. However, if the axial and bending motions are in phase, the net result would be rectilinear motion at either beam tip. By vibrating the base of the structure slightly away from the resonance of either beam, elliptical motion can be obtained from one of the two beam tips whilst the other beam tip will be vibrating rectilinearly and out-of-phase with respect to the other beam tip by approximately 90°, promoting motion in one direction. This is shown in Fig. 18.

The actuator gave a sliding velocity of 100 mm/s and 12 mN sliding force in either direction. A peak of 212 mm/s and 44 mN were obtained. By reducing the length of the applied signal, the sliding distance was reduced to 90 ± 2 nm. An indication of the scale of the device can be seen in Fig. 19. Friend et al. [35] then further reduced the scale of this design, meeting Feynman's original 1/64-in. challenge made in 1959 [36]. At these small scales, the actuator produced outputs of 40 mm/s and 30 mN in either direction.

An alternative to linear actuators using planar bending motion is the SQUIGGLE®[1] motor produced by New Scale Technologies [37]. This actuator uses coupled bending modes driven by four piezoelectric elements to create a wobbling motion in a central hollow tube. Unusually however, the actuator converts this wobbling motion to a linear displacement through the use of a threaded screw. This can be seen in Fig. 20. The actuator has a maximum dimension of 6 mm and a driven shaft of 0.9 mm. It produces a force of 196 mN and a velocity of 5 mm/s.

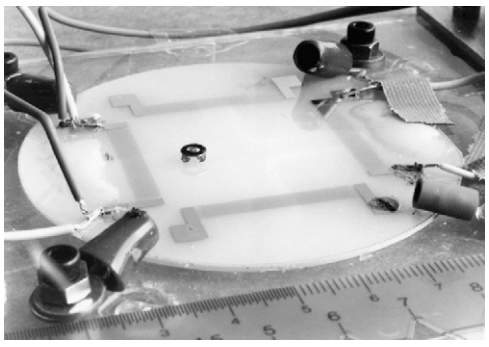

Fig. 23. The first surface acoustic wave (SAW) motor, produced by Kurosawa et al. [40]. (Figure © [1996] IEEE).

5. Propagating wave actuators

The generalised operation of a propagating wave actuator is not dissimilar from that of a standing wave design. As with standing wave designs an elliptical motion is generated in the stator, which is then transferred to the rotor through a friction coupling. The elliptical motion however, is not generated at one point within the stator; rather every point on one stator face follows an elliptical trajectory. This occurs due to the generation of the propagating wave within the stator. In general, this wave is generated by combining two standing waves, 90°out of phase. As the wave travels, particles at the surface move in an elliptical path as shown in Fig. 21. The component standing waves are generated by a pair of vibration sources, allowing the wave to propagate in both directions.

As with standing wave designs, the key characteristics of actuators in this class can be attributed to the physics involved in the operation. The small amplitude, high frequency waves generated

[1] SQUIGGLE is a registered trademark of New Scale Technologies.

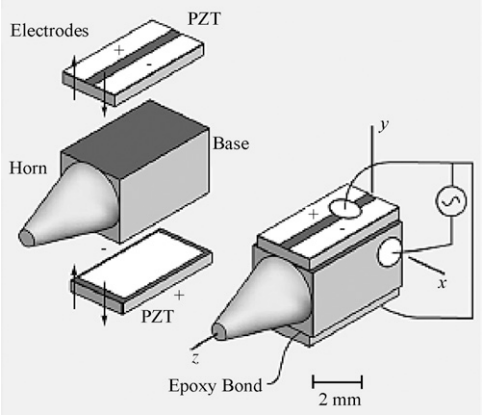

Fig. 24. The design by Friend et al. [45] uses in-plane piezoelectric bimorphs to shear the stator, resulting in a rotation at the stator tip. (Figure © [2004] IEEE).

promote high speed and high output force operation. The high frequency operation also allows a very high accuracy to be obtained from the rotor or slider, with the potential for sub-nanometre positioning accuracy [38]. However, the amplitude of the propagating wave and the complex design used to generate them both have a detrimental effect on the scalability of these designs. The amplitude of the wave produced by the device reduces linearly with the scale of the device. As we approach a sub-millimetre scale actuator, the vibration amplitude becomes so small as to become difficult to use as a driving mechanism in an actuator. In addition, the necessity to fabricate complex interdigital transducers for surface acoustic wave actuators at scales small enough to produce a sub-millimetre actuator also limits the potential for a reduction in scale for this particular class of propagating wave actuators. As such, no significant micro/milli-scale actuators have been developed in this class. Here we review some of the most successful larger scale designs and those that provide high accuracy.

5.1. Rotational actuators

The most successful type of rotary propagating wave actuators are known as "surfing" motors. In these motors, multiple vibration sources are used to excite an elastic ring. A standing wave is generated for each vibration source, and through superposition of these waves, it is possible to create a propagating wave around the ring.

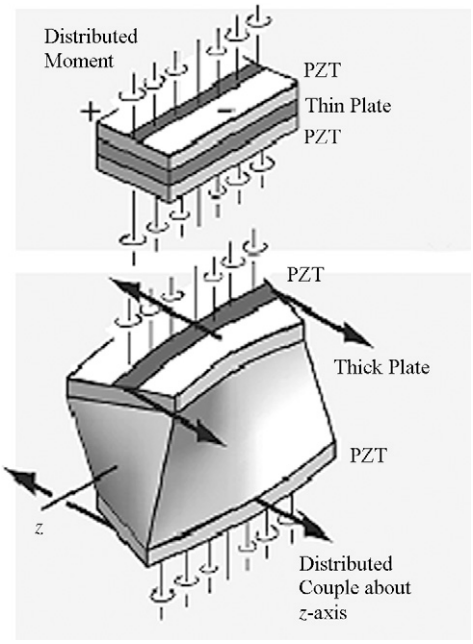

Fig. 25. Induced net moment due to the shearing effect of the piezoelectric material for the actuator proposed by Friend et al. [45]. (Figure © [2004] IEEE).

The most successful of this type of design, and arguably the most successful piezoelectric actuator ever produced, was developed by Sashida [39]. In this actuator, the travelling wave is induced in a thin piezoelectric ring, with directional reversibility achieved through an exchange of sine and cosine input voltages. Bonded to the piezoelectric element is a ring-shaped elastic body. This body was then in contact with the ring-shaped slider. This is illustrated in Fig. 22.

With a propagating wave frequency of 44 kHz and an input voltage of 10.3 V, the actuator developed a maximum torque of approximately 100×10^3 μ Nm and a maximum rotational velocity of greater than 30 rpm [22].

The performance of these surfing motors was excellent. The use of multiple input voltages to create multiple standing waves made them very controllable and high output actuators. However, as mentioned above, the complexity of the design currently limits their reduction to sizes to a scale of a few millimetres.

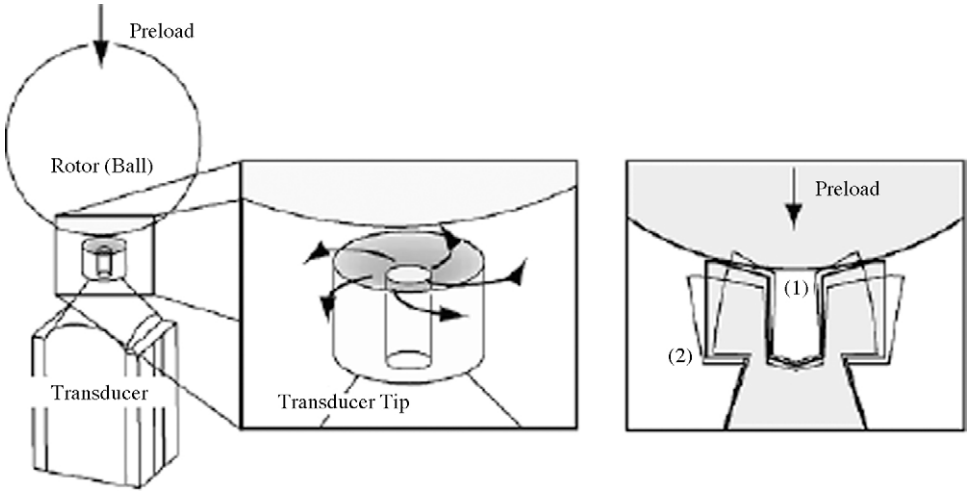

Fig. 26. Novel transducer tip design by Friend et al. The radial movement of the stator tip varies the contact force, replacing the need for an elliptical stator tip motion. The preload was produced by the weight of the ball [46].

Table 2
Comparison of the performance of rotational micro/milli-scale actuators.

Design	Driving force	Class	Motion	Actuator principle	Stator type	Stator dia. (mm)	Stator length (mm)	Output (μNm)	Velocity (rpm)
Dubois and Muralt, 1998 [29]	Converse piezoelectric effect	Standing wave	Rot.	Flexural mode	Membrane-like, elastic fins, bulk PZT	5.2	N/A	0.94	1020
Morita et al., 1999 [20]	Converse piezoelectric effect	Standing wave	Rot.	Orthogonal bending modes	Bulk PZT tube	2.4	10	220	650
Morita et al., 2000 [21]	Converse piezoelectric effect	Standing wave	Rot.	Orthogonal bending modes	Thin-film PZT on tube	1.4	5	0.67	680
Kanda et al., 2004 [17]	Converse piezoelectric effect	Standing wave	Rot.	Orthogonal bending modes	Bulk PZT	0.8	2.2	0.025	3850
Zhang et al., 2006 [24]	Converse piezoelectric effect	Standing wave	Rot.	Orthogonal bending modes	Bulk PZT tube	1	5	7.8	3000
Koc et al., 2002 [30]	Converse piezoelectric effect	Standing wave	Rot.	Degenerate ortho. bending modes	Tube with two flattened sides for bulk PZT	2.4	10	1.8×10^3	573
Yao et al., 2001 [26]	Converse piezoelectric effect	Standing wave	Rot.	Axial/bending	PZT MPLA	3	N/A	127.5	1070
Suzuki et al., 2000 [32]	Converse piezoelectric effect	Standing wave	Rot.	Axial/bending	Bulk PZT on stainless steel	2	0.3	3.2	1500
Aoyagi et al., 2004 [27]	Converse piezoelectric effect	Standing wave	Rot.	Axial/bending	Bulk PZT on stainless steel vibrator	16.2×2.5	0.55	60	8000
Tamura et al., 2008 [28]	Converse piezoelectric effect	Standing wave	Rot.	Axial/bending	Crystal anisotropy in $LiNbO_3$	10×2.55	0.5	25 CCW	5000 CW
Watson et al., 2008 [34]	Converse piezoelectric effect	Standing wave	Rot.	Torsion/axial	Helically cut tube	0.25	1	0.013	1300
Friend et al., 2004 [46]	Converse piezoelectric effect	Ultrasonic disp.	Rot.	In-plane shearing	Bulk PZT on phosphor bronze	3×4	8.5	100	425

Table 3
Comparison of the performance of linear micro/milli-scale actuators.

Design	Driving force	Class	Motion	Actuator principle	Stator type	Stator dim. (mm × mm)	Stator length (mm)	Output (mN)	Velocity (mm/s)
Friend et al., 2006 [18]	Converse piezoelectric effect	Standing wave	Linear	Bending and vertical mode coupling	Asymmetrical fins on bulk PZT	3.25 × 2.5	2	44	212
SQUIGGLE® [37]	Converse piezoelectric effect	Standing wave	Linear	Othogonal bending mode coupling	Threaded screw and bulk PZT	1.55 × 1.55	6	196	5
Shigematsu and Kurosawa, 2006 [38]	Converse piezoelectric effect	Prop. wave	Linear	SAW from IDT	Lithium Niobate	2.5 × 3	12.5	13	300

5.2. Linear actuators

The most promising of the linear propagating wave actuators are the surface acoustic wave (SAW) actuators. A SAW is an acoustic wave that travels along the surface of an elastic material. If the SAW is generated on a piezoelectric substrate (usually Lithium Niobate—$LiNbO_3$) the acoustic energy can be converted to a mechanical displacement. This displacement occurs at each particle on the surface and takes the form an ellipse as already discussed.

The first actuator using SAW as a driving force was reported by Kurosawa et al. in 1996 [40]. The design was based on a Ø76.2 mm Lithium Niobate substrate. The actuator incorporated four interdigital transducers (IDT's), allowing motion in the *x*- and *y*-directions. The driving frequency was approximately 9 MHz and produced a lateral transfer speed of 200 mm/s. An image of the device can be seen in Fig. 23.

The design was improved through the use of a multiple contact stator [41], and improved contact conditions [42] to the point where the actuator could be operated at 70 MHz and produced a transfer speed of 700 mm/s. The reduction in scale of the actuator was also examined by Takasaki et al., who produced an actuator with dimensions of 15 mm × 60 mm × 1 mm [43].

The excellent positioning accuracy of this actuator was demonstrated by Shigematsu et al. [44]. With a 60 mm × 15 mm × 1 mm $LiNbO_3$ substrate and a 9.6 MHz driving force, a stepping drive of 2 nm steps produced a 1-nm friction driven step. The authors reported that there was a potential for a sub-nanometre friction driven step. The most recent published work by Shigematsu and Kurosawa has further reduced the size of the actuator to using a 3 mm × 12.5 mm × 2.5 mm substrate and a 100 MHz driving frequency [38].

SAW linear actuators have great potential as positioning devices with nanometre accuracy or better. They also have a high output speed and good output force making them suitable for a wide range of applications. However, it will prove difficult to continually reduce the scale of the device due to the necessity to manufacture the IDT's. Moreover, SAW based actuators suffer from high wear rates stemming from the direct contact between the slider and the fragile piezoelectric material at high operating frequencies. These drawbacks of SAW propagation remain a hurdle to their commercialisation.

6. Ultrasonic displacement actuators

Ultrasonic displacement actuators use the displacement of the piezoelectric element and stator, cycled at ultrasonic frequencies, to create a useful output at the rotor or slider. These designs differ from those previously discussed as no wave is set-up within the stator to assist with the performance or to convert the piezoelectric output to a more useful form. Instead, the piezoelectric output is either converted into a linear or a rotational output at the rotor though geometrical design. Limited research has been carried out in this class for micro/milli-actuators, however, we will note one design here. The design by Friend et al. [45], which uses a shearing action to drive a rotational piezoelectric ultrasonic actuator.

This design used multiple electrodes for a bulk piezoelectric element to effectively create an in-plane bimorph. The bulk piezoelectric elements were epoxy bonded to a phosphor bronze structure that included a tapered conical horn that acted as the stator tip, as shown in Fig. 24. By applying a voltage to the correct electrodes, an in-plane shearing motion could be achieved in the piezoelectric elements. This shearing motion led to a net moment at the conical tip. This can be seen in Fig. 25.

The actuator was operated at 192.1 kHz. At this frequency and 27.3 V_{RMS}, a rotational velocity of 71 rpm was obtained at the

1.5 mm-diameter tip. At 1.02 MHz and 17.8 V_{RMS}, 371 rpm was measured at the tip.

Friend et al. also made a modification to this actuator, introducing a unique concept for translating the stator motion to the rotor [46]. By tapering the hole, as shown in Fig. 26, the tapered surface moved away from the rotor as the tip expanded outward, lowering both the contact force and the delivered torque.

The revised actuator was operated at two frequencies: 186.3 kHz for counter-clockwise motion and 246.6 kHz for clockwise motion. With a preload of 87.1 mN, a torque of 100 μ Nm was obtained with a rotational velocity 425 rpm. The overall efficiency peaked at more than 40%.

This design proposed an interesting stator set-up, and showed the potential of the system. However, the results were obtained in the absence of a practical rotor and preload system. It is also worth noting that this design requires a stator manufactured from a material with a low material damping loss. Attempts to use biocompatible tantalum in place of phosphor bronze were unsuccessful. The design may also benefit from being operated at the torsional resonance frequency of the stator, potentially improving the stator tip response.

7. Actuator performance classification

As has been noted throughout this review, classifying micro/milli-scale actuators according to their basis of operation provides an understanding of the actuator performance. This has benefits in determining successful designs, suitability for applications and further research areas. In Tables 2 and 3 we summarise the performance data of the actuators reviewed according to classification to further highlight this relationship and to provide an easy reference for review.

8. Future research areas

The next logical step of research in this field will be to develop a practical sub-millimetre scale actuator, a true micro-actuator. There is already a demand for such actuators in the micro-robotics industry [1] and the medical profession, specifically for minimally invasive surgery [2,3]. To achieve this goal, we anticipate that research will focus on the driving mechanisms that are best suited to a continued reduction in scale. From this review, it can be seen that those designs that use a resonant mode to induce a standing wave are well suited for micro-applications, and as such, will continue to be an active area of research.

In addition to the research into driving mechanisms and stator design, the other components of the actuators will also need further development. Further research into thin-film, polymer and other technologies that provide designers with smaller and better piezoelectric elements will be required. We also envisage continuing work in the areas of micro-fabrication to allow these new micro-actuators to be successfully constructed. Aside from the size reduction of actuators, further investigation needs to be conducted to improve actuator efficiencies. Current efficiencies for ultrasonic milli-actuators are around 20%. Improvements in the understanding of rotor/stator interface and friction coupling could potentially increase these efficiencies leading to a better performing actuators.

References

[1] J. Bardina, R. Thirumalainambi, Micro-Flying Robotics in Space Missions, SAE International, 2005.
[2] E.J. Hanly, M.A. Talamini, Robotic abdominal surgery, The American Journal of Surgery 188 (2004) 19S–26S.
[3] A. Menciassi, M. Quirini, P. Dario, Microrobotics for future gastrointestinal endoscopy, Minimally Invasive Therapy and Allied Technologies 16 (2007) 91–100.
[4] K. Hori, T. Miyagawa, L. Ito, Development of ultra-small sized servo actuator with brushless DC motor planetary gear drive and optical rotary encoder, International Journal of the Japan Society for Precision Engineering 31 (1997) 1–5.
[5] C.K. Malek, V. Saile, Applications of LIGA technology to precision manufacturing of high-aspect-ratio micro-components and systems: a review, Microelectronics Journal 35 (2004) 131–143.
[6] K.E. Drexler, Productive nanosystems: the physics of molecular fabrication, Physical Education 40 (2005).
[7] M. Mehregany, P. Nagarkar, S.D. Senturia, J.H. Lang, Operation of microfabricated harmonic and ordinary side-drive motors, in: Proceedings of the IEEE Micro-Electro-Mechanical Systems Workshop, February 11–14, 1990, pp. 1–8.
[8] A.M. Fennimore, T.D. Yuzvinsky, M.S. Wei-Qiang Han, J. Fuhrer, A. Cumings, Zettl, Rotational actuators based on carbon nanotubes, Nature 424 (2003) 408–410.
[9] R. Yeh, S. Hollar, K.S.J. Pister, Single Mask, Large force, and large displacement electrostatic linear inchworm motors, Journal of Microelectromechanical Systems 11 (2002) 330–336.
[10] S. Heo, Y.Y. Kim, Optimal Design, Fabrication of MEMS rotary thermal actuator, Journal of Micromechanics and Microengineering 17 (2007) 2241–2247.
[11] M.J. Sinclair, The Seventh Intersociety Conference on Thermal and Thermomechanical Phenomena in Electronic Systems (2000) 127–132.
[12] Y.-C. Su, L. Lin, A.P. Pisano, A water-powered osmotic microactuator, Journal of Microelectromechanical Systems 11 (2002) 736–742.
[13] S. Yokota, A. Sadamoto, Y. Kondoh, Y. Otsubo, K. Edamura, A micro motor using electroconjugate fluids (ECFs), JSME International Journal Series C 44 (2001) 756–762.
[14] S. Yokota, K. Kawamura, K. Takemura, K. Edamura, A High-integrated micromotor using electro-conjugate fluid (ECF), Journal of Robotics and Mechatronics 17 (2005) 142–148.
[15] S. Yokota, Personal correspondence, October 2008.
[16] L. Frank, J. Lee, Camera with electronic flash and piezoelectric lens motor, U.S. Patent Number 4,291,958, September 1981.
[17] T. Kanda, A. Makino, L. Suzumori, T. Morita, M.K. Kurosawa, A cylindrical micro ultrasonic motor using a micro-machined bulk piezoelectric transducer, in: IEEE Ultrasonics Symposium, Montreal, QC, Canada, August 23–27, 2004, pp. 1298–1301.
[18] J. Friend, Y. Gouda, K. Nakamura, S. Ueha, A simple bidirectional linear microactuator for nanopositioning—the "Baltan" microactuator, IEEE Transactions on Ultrasonics, Ferroelectrics, and Frequency Control 53 (2006) 1160–1168.
[19] T. Morita, M.K. Kurosawa, T. Higuchi, An ultrasonic micromotor using a bending cylindrical transducer based on PZT thin-film, Sensors and Actuators A 50 (1995) 75–80.
[20] T. Morita, M.K. Kurosawa, T. Higuchi, Cylindrical micro ultrasonic motor utilizing bulk lead zirconate titanate (PZT), Japanese Journal of Applied Physics 38 (1999) 3347–3350.
[21] T. Morita, M.K. Kurosawa, T. Higuchi, A cylindrical shaped micro ultrasonic motor utilizing PZT thin film 1.4 mm in diameter and 5.0 mm long stator transducer, Sensors and Actuators A 83 (2000) 225–230.
[22] K. Uchino, Piezoelectric ultrasonic motors: overview, Smart Material Structures 7 (1998) 273–285.
[23] T. Mortia, Miniature piezoelectric motors—review, Sensors and Actuators A 103 (2002) 291–300.
[24] H. Zhang, S. Dong, S. Zhang, T. Wang, Z. Zhang, L. Fan, Ultrasonic micro-motor using miniature piezoelectric tube with diameter of 1.0 mm, Ultrasonics 44 (2006) e603–e606.
[25] K. Uchino, Piezoelectric Actuators and Ultrasonic Motors, Kluwer Academic Publishers, Boston, 1997.
[26] K. Yao, B. Koc, K. Uchino, Longitudinal-bending mode micromotor using multilayer piezoelectric actuator, IEEE Transactions on Ultrasonics, Ferroelectrics, and Frequency Control 48 (2001) 1066–1071.
[27] M. Aoyagi, F. Suzuki, Y. Tomikawa, I. Kano, High-speed thin ultrasonic spindle motor and its application, Japanese Journal of Applied Physics 43 (2004) 2873–2878.
[28] H. Tamura, K. Shibata, M. Aoyagi, T. Takano, Y. Tomikawa, S. Hirose, Single phase drive ultrasonic motor using $LiNbO_3$ rectangular vibrator, Japanese Journal of Applied Physics 47 (2008) 4015–4020.
[29] M.A. Dubois, P. Muralt, PZT thin film actuated elastic fin micromotor, IEEE Transactions on Ultrasonics, Ferroelectrics, and Frequency Control 45 (1998) 1169–1177.
[30] B. Koc, S. Cagatay, K. Uchino, A piezoelectric motor using two orthogonal bending modes of a hollow cylinder, IEEE Transactions on Ultrasonics, Ferroelectrics, and Frequency Control 49 (2002) 495–500.
[31] K. Uchino and K. Ohnishi, Linear motor, U.S. Patent Number 4,857,79, August 1989.
[32] Y. Suzuki, K. Tani, T. Sakuhara, Development of a new type piezoelectric micromotor, Sensors and Actuators A 83 (2000) 244–248.
[33] S. Mishiro, Rotary ultrasonic motor, U.S. Patent Number 4,697,117, September 1987.
[34] B. Watson, J. Friend, L. Yeo, Piezoelectric ultrasonic resonant motor with stator diameter less than 250 μm: the Proteus motor, Journal of Micromechanics and Microengineering 19 (2009) 022001–022005.
[35] J. Friend, L. Yeo, M. Hogg, Piezoelectric ultrasonic bidirectional linear actuator for micropositioning fulfilling Feynman's criteria, Applied Physics Letters 92 (2008) 0141071–0141073.
[36] R. Feynman, There's plenty of room at the bottom, Journal of Microelectromechanical Systems 1 (1992) 60–66.

[37] D.A. Henderson, Simple ceramic motor.. inspiring smaller products, actuator 2006, in: 10th International Conference on New Actuators, Bremen, Germany, June 14–16, 2006.
[38] T. Shigematsu, M.K. Kurosawa, Miniaturized SAW motor with 100 MHz drive frequency (letter), IEEJ Transactions on Sensors and Micromachines 126 (2006) 166–167.
[39] T. Sashida, Motor device utilizing ultrasonic oscillation, U.S. Patent Number 4,562,374, December 1985.
[40] M. Kurosawa, M. Takahashi, T. Higuchi, Ultrasonic linear motor using surface acoustic waves, IEEE Transactions on Ultrasonics, Ferroelectrics, and Frequency Control 43 (1996) 901–906.
[41] M.K. Kurosawa, M. Chiba, T. Higuchi, Evaluation of a surface acoustic wave motor with a multi-contact-point slider, Smart Material Structures 7 (1997) 305–311.
[42] M. Takasaki, M.K. Kurosawa, T. Higuchi, Optimum contact conditions for miniaturized surface acoustic wave linear motor, Ultrasonics 38 (2000) 51–53.
[43] M. Takasaki, N. Osakabe, M.K. Kurosawa, T. Higuchi, Miniturization of surface acoustic wave linear motor, in: IEEE Ultrasonics Symposium, Sendai, Miyagi, Japan, October 5–8, 1998, pp. 679–682.
[44] T. Shigematsu, M.K. Kurosawa, K. Asai, Nanometer stepping drives of surface acoustic wave motor, IEEE Transactions on Ultrasonics, Ferroelectrics and Frequency Control 50 (2003) 376–385.
[45] J. Friend, K. Nakamura, S. Ueha, A torsional transducer through in-plane shearing of paired planar piezoelectric elements, IEEE Transactions on Ultrasonics, Ferroelectrics, and Frequency Control 51 (2004) 870–877.
[46] J. Friend, K. Nakamura, S. Ueha, A piezoelectric micromotor using in-plane shearing of PZT elements, IEEE/ASME Transactions on Mechatronics 9 (2004) 467–473.

Biographies

Brett Watson is currently undertaking his Ph.D. degree in Mechanical Engineering at Monash University as part of the MicroNanophysics Research Laboratory. He received his Bachelor of Engineering (Mechanical) from Curtin University in 2000. His research interests are in motors, actuators and propulsion systems for biomedical micro- robotic applications. His paper on a piezoelectric micro-motor for in vivo swimming microbots at AOTULE 2008 was highly commended, he is a member of the Golden Key Honour Society and currently has a patent application in progress.

James Friend (member IEEE) received the B.S. degree in aerospace engineering, and the M.S. and Ph.D. degrees in mechanical engineering from the University of Missouri-Rolla in 1992, 1994, and 1998, respectively. He received two awards—the AIAA Jefferson Student Goblet and ASME Presentation Award—for his presentation on ultrasonic motor analysis at the AIAA/ASME/AHS/ASC 26th Annual Structural Dynamics Conference in 1996, an award for the encouragement of young scientists at the Symposium for Ultrasonic Electronics and Engineering in 2003 for a presentation on acoustic waveguides, an award in 2004 for a presentation on the Scream actuator at the Spring Meeting of the Acoustical Society of Japan, excellence in teaching and early career researcher awards from the Monash Faculty of Engineering in 2007 and 2008, respectively, and a Future Leader award from the Davos Future Summit in Sydney in 2008. James Friend joined Monash University in late 2004, and founded and co-directs the $6.5 million MicroNanophysics Research Laboratory with clean room and biolab, a current staff of three academics, three post-doctorates and thirteen PhD students. He is an associate professor and deputy head of the Department of Mechanical and Aerospace Engineering at Monash University, with research interests in micro/nanodevices for biomedical applications, with over one hundred peer-reviewed publications, with five book chapters, fifty-two peer-reviewed journal papers, and thirteen patents and patent applications.

Dr Leslie Yeo is currently an Australian Research Fellow and Senior Lecturer in the Department of Mechanical & Aerospace Engineering and Co-Director of the Micro/Nanophysics Research Laboratory at Monash University, Australia. He received his PhD from Imperial College London in 2002, for which he was awarded the Dudley Newitt prize for a computational/theoretical thesis of outstanding merit. Prior to joining Monash University, he was a Mathematical Modeller at Det Norske Veritas UK and a postdoctoral research associate in the Department of Chemical & Biomolecular Engineering at the University of Notre Dame, USA. Dr Yeo was the recipient of the 2007 Young Tall Poppy Science Award from the Australian Institute for Policy & Science 'in recognition of the achievements of outstanding young researchers in the sciences including physical, biomedical, applied sciences, engineering and technology', and a finalist in the 2008 Eureka Prize People's Choice Award. Dr Yeo is the author of over 70 research publications and over 10 patent applications, and is currently the Associate Editor of the American Institute of Physics journal Biomicrofluidics.